

# Impact of Carbon Nanotubes Reinforcement on Microstructural and Tribological Characteristics of Air Plasma Sprayed Conventional Alumina-Titania ( $\text{Al}_2\text{O}_3$ -3wt% $\text{TiO}_2$ ) Coatings

G. M. Thalib Basha and V. Bolleddu\*

\* venkateshwarlu.b@vit.ac.in

Received: March 2020

Revised: May 2020

Accepted: June 2020

School of Mechanical Engineering, Vellore Institute of Technology, Vellore, Tamilnadu, India.

DOI: 10.22068/ijmse.17.3.92

**Abstract:** The microstructural characteristics, mechanical properties and wear characterization of air plasma sprayed coatings obtained from Carbon nanotubes (CNTs) reinforced  $\text{Al}_2\text{O}_3$ -3wt% $\text{TiO}_2$  powders were examined at different loading conditions and different percentage proportion of CNTs. The CNTs in the proportion of 2, 4, and 6 wt% were used as nanofillers to modify the properties of coatings. The uniform dispersion of CNTs throughout the powder particles can be observed from the SEM micrographs. The porosity of the microstructure of the coatings was measured by image analysis. Also, the mechanical properties such as microhardness and surface roughness were measured by microhardness tester and profilometer, respectively. The wear tribometer was used to analyze the tribology of the coatings by varying different parameters. The different loading conditions used were low load (0.5 kgf), moderate load (1.0 kgf), and elevated load (1.5 kgf), respectively. The microhardness showed a slight increase with an increase in the percentage of CNTs proportion. Similarly, the surface roughness value showed a decreasing trend, since the CNTs were filled in the pores. From wear tests, it was observed that the coefficient of friction and wear rate were very less at 6wt% CNTs and 1.5 kgf load. This was mainly due to the bridging of CNTs in between the splats. This implies that CNTs were one of the most suitable additives for improving the microstructural and tribological characteristics of the ceramic coatings.

**Keywords:** Carbon nanotubes (CNTs); Wear Behavior; Coefficient of Friction (COF); CNT bridging.

## 1. INTRODUCTION

The plasma sprayed coatings were extensively used for wear resistance applications such as turbine blades, plunger pumps, the lining of aircraft engines, etc., [1-2]. These coatings possess extreme microhardness and good modulus of elasticity [3]. Alumina-titania powders were widely used feedstock to obtain the plasma sprayed coatings for their excellent wear resistance [4]. In many structural and dynamic applications,  $\text{Al}_2\text{O}_3$ - $\text{TiO}_2$  was mainly used for improving the surface properties [5]. Even though alumina-titania ceramic coatings possess many advantages, some critical issues resist their application such as brittle nature due to which coatings may fail. This phenomenon was attributed to the fracture of coatings due to abrasion at high loads. Also, the ceramic coatings lack in the formation of a protective layer that reduces the coefficient of friction. In the field of tribological behavior, many researchers had done several experiments to enhance the wear resistance and reduction of friction on the ceramic coatings.

The multiwalled carbon nanotubes (MWCNTs) were gaining popularity recently due to their ability in improving the mechanical properties of coatings obtained from the thermal spraying process [6]. However, carbon nanotubes (CNTs) are considered as an exceptional choice for reinforcement of ceramics with their superior properties such as physical microstructure and mechanical strength. CNTs were also having a high elastic modulus of 1000 GPa, the high tensile strength of 60 GPa, and thermal conductivity of 3000 W/mK [7]. Generally, the plasma sprayed coating system possesses a topcoat and the bond coat. The bond coat had various issues in functioning mainly due to the variation in the thermal expansion coefficient [8]. By adding CNTs to  $\text{Al}_2\text{O}_3$ + $\text{TiO}_2$  ceramic powders, the mismatch in thermal expansion is reduced [9]. CNTs also possess unique mechanical features due to their geometry and size. However, it cannot be used directly without any percentage composition, since it also suffers from a few limitations like agglomerating the powder to resist from free flow during the coating process. Also, excessive carbon may create damage to the

coatings at higher temperatures. Therefore, it is required to maintain some pre-requisite composition of CNTs to be mixed with coating powders to acquire toughness of matrix using standard mechanical mixing process like ball milling [10-14].

The various reinforcements such as CNTs, graphene oxides, yttria oxide ( $Y_2O_3$ ),  $TiO_2$ ,  $Bi_2O_3$ , diamond, etc., were added to the alumina-titania coatings to improve properties such as toughness, microhardness, and wear resistance. The reinforcement of 20wt% of  $Y_2O_3$  to  $Al_2O_3$ -13wt% $TiO_2$  coatings result in improved densification, stabilization of  $\alpha$ -phase, and enhancement in toughness due to fracture [15]. The bi-modal microstructure due to the addition of  $TiO_2$ ,  $Bi_2O_3$  possesses a lubricating layer by the formation of  $NiTiO_3$  and  $Al_2TiO_5$  layer which improves the tribological properties [16].

The microstructural properties of alumina coatings were examined by Psyllaki *et al* (2001), in which it was showed that alumina-titania coatings with denser microstructure possess better wear resistance as compared to the coating with more number of pores [17]. The dependence of wear characteristics on the microstructural properties was conducted by Hawthorne *et al* (1997). The inter-splat cohesion and porosity harm the microhardness and the increase in splat size improves the microstructural properties of the coatings [18]. The addition of a small quantity of MWCNTs to the Mg alloy results in the improvement of tensile strength and yield stress. Also, the splats size increases with the addition of CNTs which leads to the improvement of microstructural properties. The reinforcement of CNTs to the  $Al_2O_3$  coatings enhance the hardness to 8.4% and toughness of the coatings to 21.1% [19].

The tribological characteristics of the CNT reinforced  $Al_2O_3$  composite coatings were studied previously [20]. Ahmad *et al.* (2010) examined the wear characteristics of  $Al_2O_3$  mixed with CNT composites using  $Si_3N_4$  ball with variation in percentage composition of CNTs up to 10%. The enhancement of wear resistance was found mainly due to the bridging of CNTs present in between  $Al_2O_3$  splats. This phenomenal change resulted in the strengthening of grain boundaries [21]. Similarly, An *et al.* (2003) investigated the wear resistance of  $Al_2O_3$  composites reinforced

with CNTs and found that  $Al_2O_3$  composites with 4wt% CNTs reinforcement showed good wear resistance characteristics. It was also found that with the increase in CNTs percentage, there was a fall in wear resistance at 10 wt. % of CNTs addition [22]. In other work, it was also observed that due to the homogeneous dispersion of CNTs, the wear performance was improved [23]. The tribological performance was also conducted by Sudhakar Jambagi C *et al* (2019), in which the CNTs were mixed by a hetero-coagulation method. The wear tests were performed by a pin-on-disc tribometer, which provides the detail of a decrease in coefficient of friction and loss of mass due to wear with increasing in the percentage of CNTs. It was also showed that due to the addition of CNTs, the hardness and toughness of the coatings were improved. The improvement in wear resistance was mainly due to the presence of CNT bridging connects the intersplats and resists the sliding of coated material during the tribo-action [24].

In this present work, the wear behavior of CNTs reinforced coatings derived from Air Plasma Sprayed Conventional  $Al_2O_3$ -3wt% $TiO_2$  powders were examined at room temperature. Even though nanostructured powders provide very good results in terms of wear resistance, microhardness, etc., we were using conventional powders since very little data was available related to coatings obtained from CNTs mixed conventional Alumina-Titania powders. The percentage proportion of CNTs present in the  $Al_2O_3$ -  $TiO_2$  composite coating system varied as 2, 4, and 6 wt. %. The wear tests were conducted using the ball-on-disc tribometer. The main objective of this work is to study the wear characteristics of the coatings at different load, speed, and time conditions and also to analyze the wear mechanisms involved.

## 2. EXPERIMENTAL PROCEDURE

### 2.1. Coating and Sample Preparation

In this work, CNT reinforced  $Al_2O_3$ -3wt%- $TiO_2$  ceramic powder was sprayed thermally through the Air Plasma Spraying process to obtain the coatings. The microstructural, mechanical, and wear characteristics of these coatings were examined by varying the percentage com-

position of CNTs with 2wt%, 4wt%, and 6wt% respectively. The Alumina-3wt%Titania powders and MWCNT powders were purchased from *Nano Research Lab, Jamshedpur, Jharkhand, India*. Then the  $Al_2O_3$ -3wt% $TiO_2$  (AT) powders of (Particle size: 40-45 $\mu$ m; Density: 3.64 g/cm<sup>3</sup>) were mixed using Ball milling process of different weight percentage of CNTs of (Diameter: 95-125nm; Length: 5-10 $\mu$ m; Density: 1.6g/cm<sup>3</sup>) 2wt% (i.e., [100grams AT+20grams CNTs]), 4wt%(i.e., [100grams AT+40grams CNTs]) , and 6wt% (i.e., [100grams AT+60grams CNTs]). The average density of  $Al_2O_3$ -3wt% $TiO_2$  reinforced with CNTs was found that 3.66-3.70 g/cm<sup>3</sup>. The mild steel substrates of AISI 1020 (55x45x5) mm were used for the deposition of coatings due to less expense and ease of availability [25]. The surface grinder (Alex NH 500) was used to remove the excess dirt and unwanted oxide layers from the surface and also to maintain the surface roughness of the sample to be 0.1 $\mu$ m. The substrate samples were grit blasted using alumina grits of an average size 28 at an air pressure of 140 psi. Then the samples were kept in an iso-propanol solution for 30 min to remove the foreign particles completely. At last, the substrates were preheated to 180°C using a Plasma Gun. The Sulzer Metco 3MB plasma gun was used to deposit the coatings. Argon was used as the primary plasma gas, whereas hydrogen was used as the secondary plasma gas. Ni-10wt%CrAlY was used as the bond coat of thickness 150-180  $\mu$ m. The thickness of the ceramic top coating was approximately 300-350  $\mu$ m.

The various parameters used for the deposition of coatings were shown in Table.1. For analysis purposes, the specimens of 10 x 5 x 5 mm size were cut from coated samples, using a low-speed diamond saw cutter. For micrographic evaluations, hot mountings with sample inserts were prepared using of Bakelite powder using a hot mounting process. The hot mounted samples with coatings crossed section were refined using Silica-Carbide (SiC) papers of 220, 400, 600, 800, and 1000 grades. The process of polishing was carried out for 10 minutes with each abrasive paper and then disc polishing was done for 15 minutes.

**Table 1.** Parameters for Plasma Spraying Process

Parameter	Range
Voltage	50 V
Current	490 A
Flow rate of Primary Gas (Ar)	50-60 Lit/min
Flow rate of Carrier Gas (H <sub>2</sub> )	8-10 Lit/min
Powder feeding rate	40-50 gm/min
Spray distance	75-150 mm

## 2.2 Microstructural and Mechanical Tests

The microstructures of coated samples were examined using a Zeiss Evo 60 scanning electron microscope (SEM). For a specified CNT percentage, of each coating, five SEM images were obtained at a variable magnification of range 1000X to 10,000X. X-ray diffraction studies were conducted using a PANalytical X'Pert PRO PW1070 instrument with  $CuK\alpha$  radiation, operating at 40 kV voltage and 30 mA current with a scanning step of 0.0167° and step time of 0.13 s. Microhardness measurements were carried out using MMT\_X7B microhardness tester (MAT Suzawa, Japan) with a Vicker's indenter at 100 g load and 15 s dwell time. An average of ten readings was taken for each coating. The surface roughness of as-deposited coatings was also measured using a Marsurf precision profilometer and TalyProfile software. The readings were taken at selected random locations and average and the standard deviation was computed. Also, the most familiar technique to evaluate the porosity of a coating system i.e. preparing a metallographic sample and then taking multiple micrographs for analysis was done. The image analysis was carried using a contrast difference between voids i.e., pores to estimate the percentage of porosity [26]. The details on the number of samples used for analysis was 9 (i.e.,  $Al_2O_3$ -3wt% $TiO_2$ +2wt%CNTs: 3 samples,  $Al_2O_3$ -3wt% $TiO_2$ +4wt%CNTs: 3 samples,  $Al_2O_3$ -3wt% $TiO_2$ +6wt%CNTs: 3 samples). A total of 6 samples were required for conducting wear tracks with different loading, speed, and timing condition for different percentages of CNTs. And 3 samples were required for performing microstructural characterization and to conduct microhardness and surface roughness tests.

### 2.3 Ball-on-Disc Wear Test

The wear tests were performed on as-sprayed coatings using the Ducom tribometer (model: TR-20-OLE) to evaluate wear characteristics. Tests were done using different loads (0.5, 1.0 and 1.5 kgf) at different sliding speeds (0.17, 0.33 and 0.5 m/s). The sliding distance was kept constant i.e., 300 m and the Tungsten-Carbide (WC) balls of 10 mm diameter were used for all the tests. The weight loss of coated samples was calculated by measuring the sample weight before and after wear test using an electronic balance (Essae: Model: FB-600). The debris formed as a result of the wear test can be removed by the manual blowing of air over the sample. Three wear tests were performed for each load and speed condition to confirm the consistency of results. The mean and standard deviation of the obtained data for the weight loss were evaluated.

The morphology of wear tracks was observed using a ZEISS EVO 60 scanning electron microscope (SEM) to find out the wear mechanisms. The parameters for conducting wear tests were given in Table 2. The wear rate was calculated using below- mentioned relation [27],

$$W_r = V/F \cdot L$$

where  $W_r$  is the wear rate ( $\text{mm}^3/\text{N} \cdot \text{m}$ ),  $V$  is the wear volume ( $\text{mm}^3$ ),  $F$  is the normal load (N), and  $L$  is the sliding distance (m).

The wear volume ( $V$ ) can be calculated using the relation,

$$V = (\text{Weight before test} - \text{Weight after test}) / \text{Density of powder particles.}$$

The Density of used powders here was  $3.64 \text{ g/cm}^3$  (Data obtained from Nano research Lab, Jharkhand, India).

Table 2. Wear Test parameters

Test Parameter	Value
Load (N)	5 (0.5kgf), 10 (1kgf), 15 (1.5 kgf)
Distance covered (cm)	30000
Speed of sliding (m/s)	17, 33, 50
Diameter of wear track (cm)	1

## 3. RESULTS AND DISCUSSION

### 3.1. Analysis of Morphology and Phases Determination

The morphology of  $\text{Al}_2\text{O}_3$ -3wt% $\text{TiO}_2$  powder was analyzed using SEM before and after adding CNTs in the proportion of 2wt%, 4wt%, and 6wt%. The CNTs were uniformly dispersed throughout the powders. Though the tap density of ceramic powders mixed with CNTs was not calculated, it was observed that the percentage proportion of powder blown away was much higher for powders without adding CNT, but after adding CNT the tap density gets increased. The slight variation in the increase of the density indicates that the uniform distribution CNTs throughout the powder particles. It can be found that  $\text{Al}_2\text{O}_3$ -3wt% $\text{TiO}_2$  powders were regular, wedge-shaped, and also contain pores in it whereas CNTs are looking like bundle-shaped structure. The presence of CNTs in Alumina-Titania composition can be clearly seen at higher magnification (150 kX) (See Fig. 1(a and b)) [4, 28]. The schematic representation of coatings was shown in Fig.2. The optical microscopy was used to evaluate the thickness of coatings (nearly 220-240 microns) as shown in Fig.2a. The SEM image of the topcoat microstructure as shown in Fig.2b.

The XRD pattern for powder and coating were shown below in Fig. 3. The XRD analysis of  $\text{Al}_2\text{O}_3$ -3wt% $\text{TiO}_2$  powder shows the presence of  $\alpha$ -Alumina and Anatase Titania phases in it as shown in Fig. 3a. The presence of  $\alpha$ -alumina in the powder provides resistance to high temperature and very little amount of anatase titania with tetragonal crystal structure provides stability to  $\alpha$ -alumina. The phases present in  $\text{Al}_2\text{O}_3$ -3wt% $\text{TiO}_2$  coatings after adding CNTs were shown in Fig. 3b. In Alumina-Titania coatings with CNTs, the major phase observed was  $\alpha$ -alumina which was also present in the coatings without CNTs. The anatase titania phase present in the powder was transferred to Rutile and Magneli phases in the coating. The Rutile phase was the most stable form of  $\text{TiO}_2$  than the anatase phase at all temperatures. Magneli phase was obtained due to the reduction (i.e. removal of oxygen) of titania at high temperatures [29]. Since the phases were the same in 2wt%, 4wt%, and 6wt% CNT added coating systems, the XRD pattern for only 6wt% CNT doped coatings was shown in Fig. 3b.



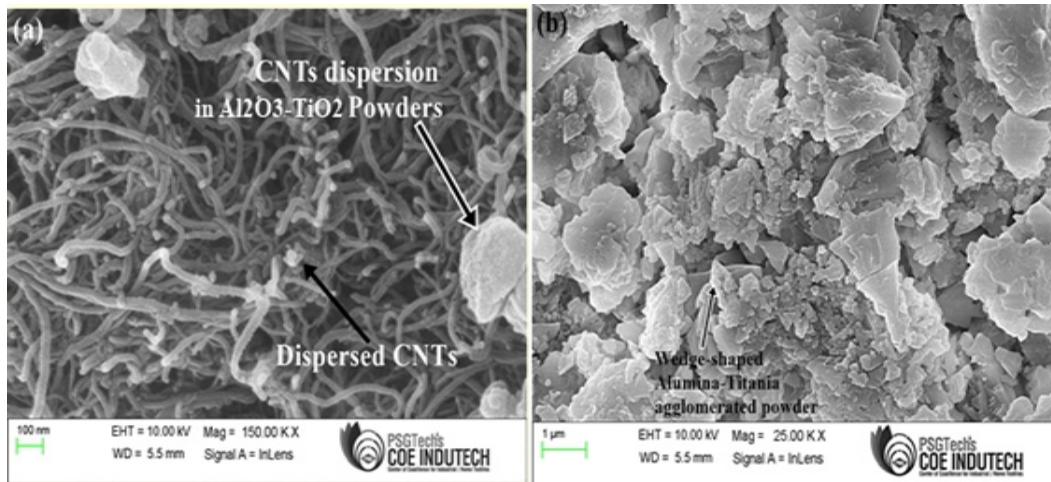


Fig. 1. Dispersion of 6wt%CNTs in Conventional  $\text{Al}_2\text{O}_3$ -3wt% $\text{TiO}_2$  (a) At higher magnification (b) At lower magnification

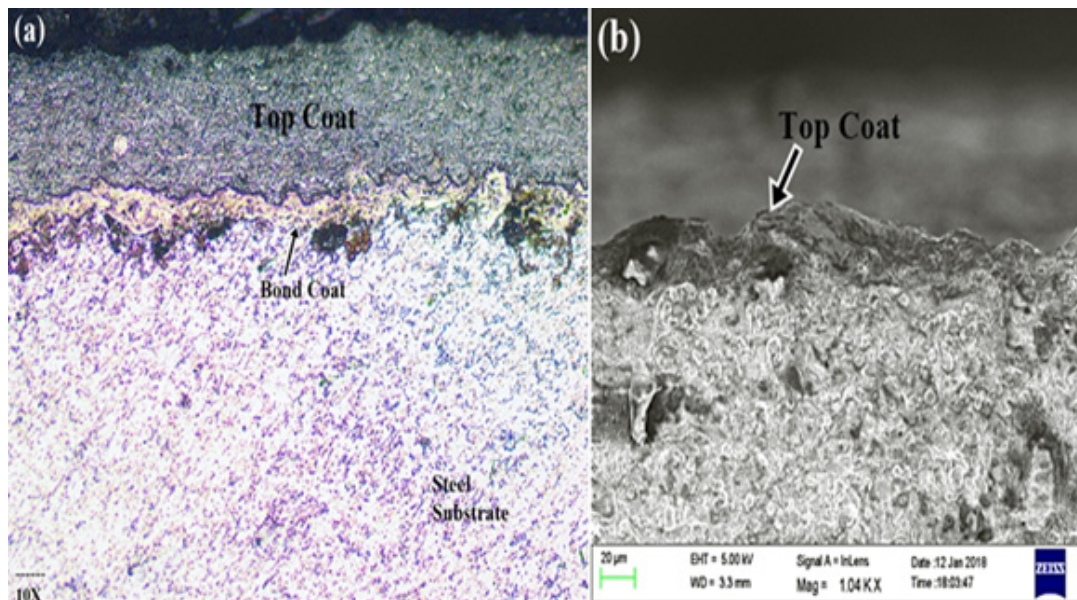


Fig.2. (a) Optical microstructure showing coating thickness representation, (b) SEM image showing topcoat microstructure

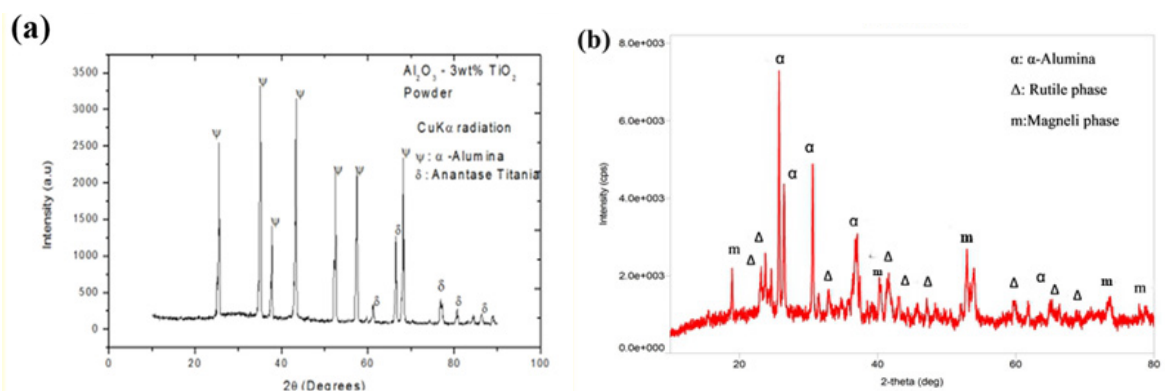


Fig. 3. XRD pattern of (a) Conventional  $\text{Al}_2\text{O}_3$ -3wt% $\text{TiO}_2$  Powder, (b)  $\text{Al}_2\text{O}_3$ -3wt% $\text{TiO}_2$  Coatings with 6wt% CNTs

### 3.2. Mechanical Properties

The microhardness tests were carried out using Vicker’s microhardness tester and the results were shown in Fig.4 (a). The microhardness is measured on the cross-section of coatings. Ten readings were taken and an average was calculated for each coating system. From microhardness graphs, it implies that the microhardness value increases slightly when the percentage of CNTs increased in the coating systems (See Fig. 4a). The results were not much varied because the percentage variation of CNT is very less (i.e. 2wt%, 4wt%, and 6wt %). The highest microhardness value of 1540.72VHN was recorded for coatings with 6wt% CNTs Shreshta Ranjan *et al.* (2019) [30, 31].

The surface roughness measurement has been carried out on the as-sprayed coatings obtained with the addition of CNTs. Six observations were recorded for each coating system and average surface roughness (Ra) was calculated. The results obtained were shown below in Fig.4 (b). It can be found that the surface roughness gets reduces with the rise in the percentage of CNTs for the coating systems (see Fig.4 b). The maximum value of surface roughness observed for the Alumina-Titania coating system with 2wt% CNTs was 6.3  $\mu\text{m}$ . The main reason for this phenomenon is that the coatings without CNTs have more number of pores on their surface and resulting in more surface roughness. When the CNTs were added to the coating systems the pores were covered and the coating surface becomes smooth. The minimum surface roughness of 5.1  $\mu\text{m}$  was observed for the coating system with 6wt% of CNT. The percentage variation of porosity with the addition of CNTs was mentioned in Fig. 4. It can also be observed that the percentage of porosity falls with the intensification of CNTs percentage. The minimum porosity of  $4.7\pm 1.2$  percent was observed for the coatings with 6wt% CNTs (see Fig. 5).

### 3.3. Wear Characterization

The tribological characteristics of coated samples were investigated and it was found

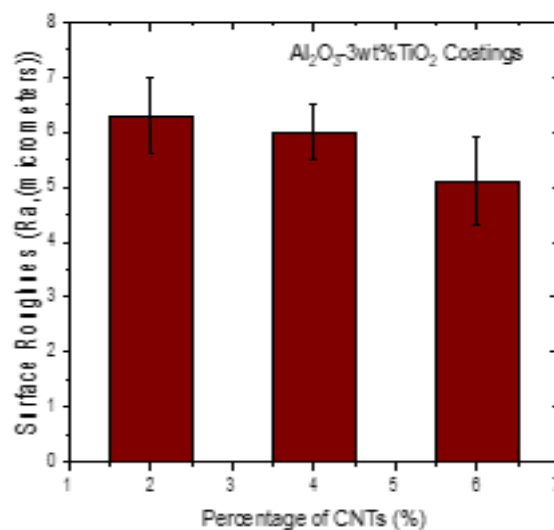
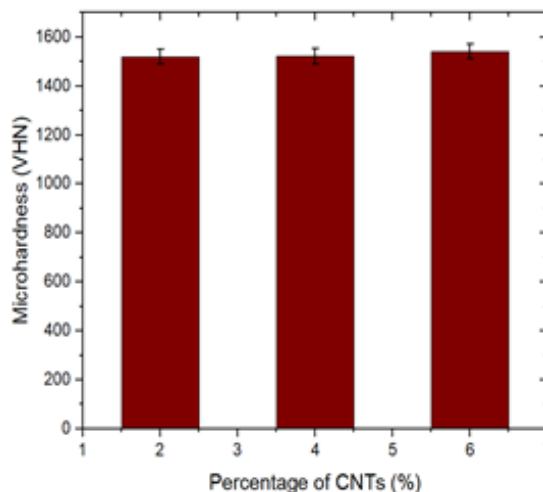


Fig. 4. Graphs of  $\text{Al}_2\text{O}_3$ -3wt% $\text{TiO}_2$  Coatings system with respect to CNT percentage (a) Microhardness, (b) Surface Roughness

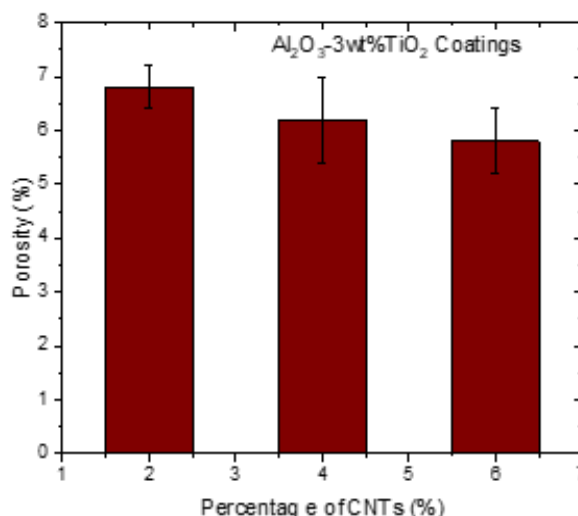


Fig. 5. Graphical representation of Porosity of coatings with respect to CNT percentage

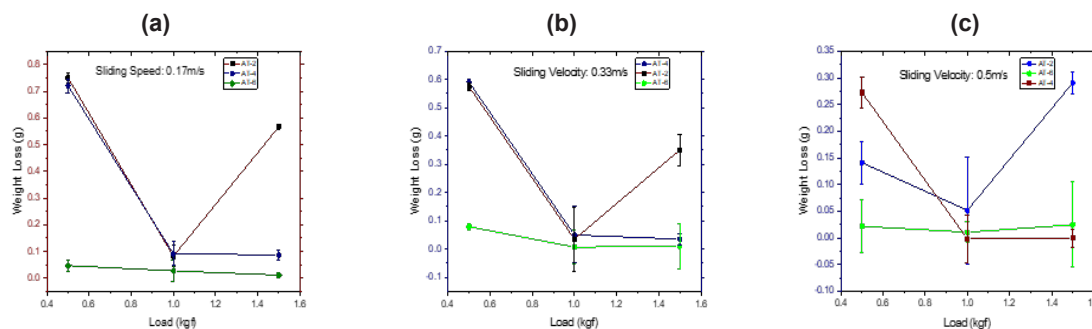


Fig. 6. Loss of weight versus different loads for Alumina-Titania Coatings with 2wt% (AT-2), 4wt% (AT-4) and 6wt% (AT-6) CNTs at a sliding velocity of (a) 0.17m/s, (b) 0.33m/s and (c) 0.5m/s.

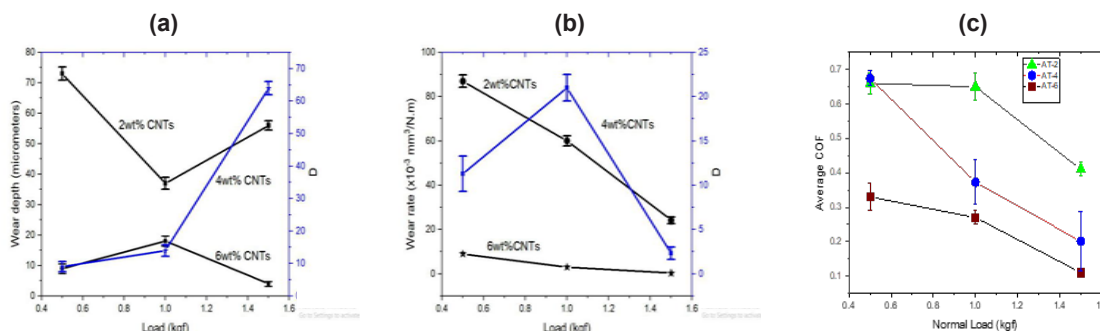


Fig. 7. (a) Load versus wear depth, (b) Load versus wear rate (c) Average Friction Coefficient (COF) versus Load for Al<sub>2</sub>O<sub>3</sub>-wt% TiO<sub>2</sub> Coatings with 2wt% (AT-2), 4wt% (AT-4) and 6wt% (AT-6) CNTs

Table 3. Ball-on-Disc Wear Test Results Analysis

Load (kgf), Sliding Velocity (m/s)	Wear Depth, $\mu\text{m}$			Wear Rate $10^{-3} \text{ mm}^3/\text{N}\cdot\text{m}$			Coefficient of friction		
	2wt% CNTs	4wt% CNTs	6wt% CNTs	2wt% CNTs	4wt% CNTs	6wt% CNTs	2wt% CNTs	4wt% CNTs	6wt% CNTs
<b>1.5, 0.17</b>	56±1.5	64±2.0	4±0.8	24.2±1.5	2.34±0.7	0.3±0.1	0.41±0.02	0.37±0.04	0.11±0.009
<b>1.0, 0.33</b>	37±2.0	14±1.8	18±1.6	60±2.3	21±1.5	3±0.3	0.65±0.04	0.45±0.03	0.27±0.02
<b>0.5, 0.5</b>	73±2.2	29±2.2	9±1.6	87±2.8	113±2.0	9±0.8	0.66±0.03	0.59±0.01	0.33±0.04

that Alumina-3wt%Titania with 6wt%CNT (AT-6) possess less wear and reduced coefficient of friction as compared to Alumina-3wt%Titania with 2wt%CNT (AT-2) and Alumina-3wt%Titania with 4wt%CNT (AT-4). The variation in weight loss with the change of normal load during wear tests was shown in Fig. 6(a-c). The change in weight loss as a function of sliding velocity follows a critical trend in all the parametric conditions due to the presence of CNT patches. It can be observed that the weight loss was less for the coated samples of AT-6 at the sliding velocities of 0.33 and 0.17 m/s except for 0.5 m/s as compared to AT-4. For these

coatings (AT-6), at the sliding velocity of 0.5 m/s, the weight loss was recorded very less (i.e., less than 0.05g) compared to the other two sliding speeds at all the loads. This phenomenon was mainly due to the presence of a rich shielding layer of CNTs over the surface of coated samples. For AT-4 samples, it was seen that the weight loss trend remains almost similar at all sliding speeds. Also, at 1.0 kgf and 1.5 kgf loads, weight loss was almost the same (see Fig. 6a-c). In a similar manner, for AT-2 samples, the weight loss was observed more at 0.5kgf and 1.5 kgf due to the presence of less amount of CNTs Liutauras *et al.* (2018) [32].



The data obtained for wear depth, wear rate, and coefficient of friction (COF) at different test parameters were provided in Fig.7 (a-c) and also in Table 3. The average coefficient of friction as a function of normal loads for AT-2, AT-4, and AT-6 was shown in Fig. 7(a-c). For the AT-6 coated samples, at the maximum loading condition of 1.5 kgf, the lowest COF of  $0.11 \pm 0.009$  and least wear volume of  $0.9 \text{ mm}^3/\text{N}\cdot\text{m}$  were found. The reason for this phenomenon was the CNTs could not be pulled out from the coatings even at higher loads. So, the unpulled CNTs act as a protective film that provides very less coefficient of friction (Jian

Rong *et al.* 2016 ) [33]. From the graph shown in Fig. 6, it can also be observed that the COF reduces with an increase in the percentage of CNT proportion.

The wear track morphologies of all the coatings (i.e., AT-2, AT-4, and AT-6) obtained at a load of 1.5kgf and at a speed of 0.17 m/s were mentioned in Fig. 8(a-f) and at this parametric conditions, the wear can be seen clearly in all the coating systems. The wear track morphology was seen rough for the AT-2 coating system since the CNTs percentage was less and hence it results in a lesser volume of the protective layer (see Fig. 8a, b). It can also be observed that the CNTs were pulverized at this max-

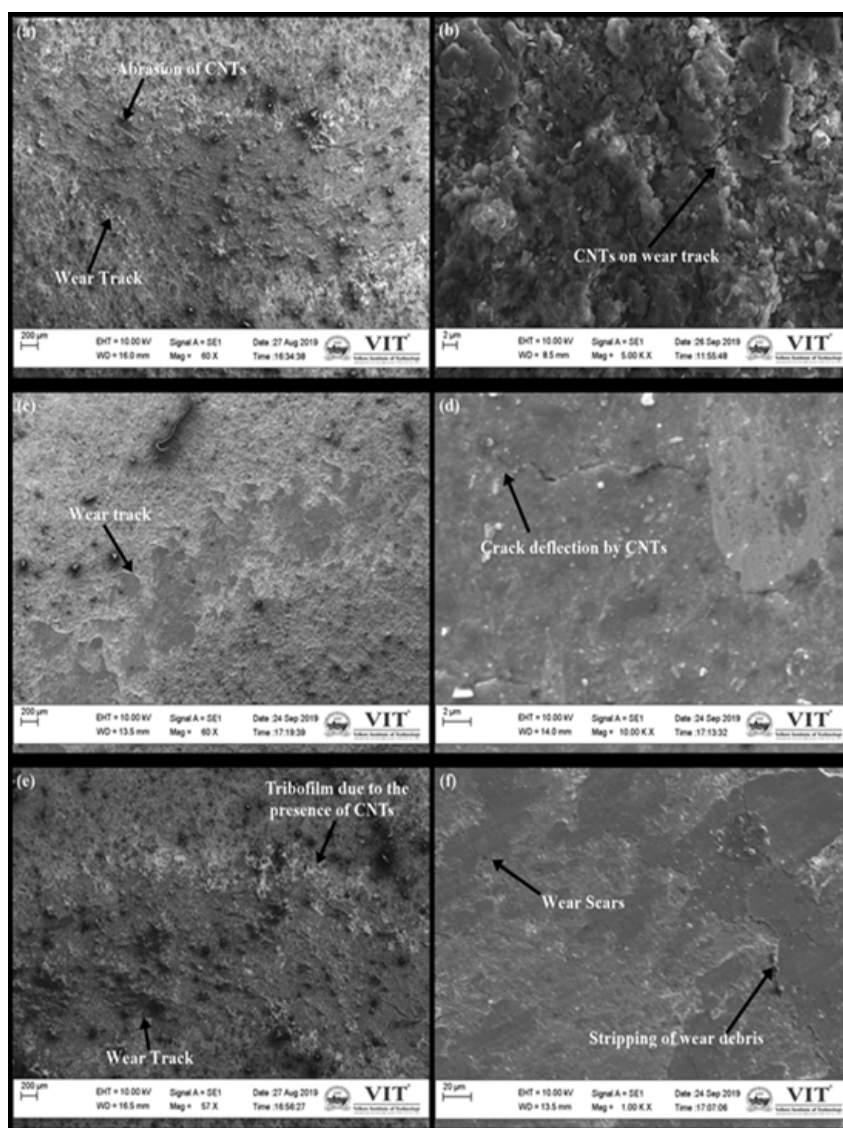


**Fig. 8.** Wear track morphology for coatings obtained from Alumina-Titania powders at different magnifications (a, b) Coatings deposited with 2wt% CNT, (c,d) Coatings deposited with 4wt% CNT and (e,f) Coatings deposited with 6wt% CNT. Micrographs shown were for a load of 1.5kgf, Sliding velocity of 0.17m/s, and a sliding distance of 300metres.



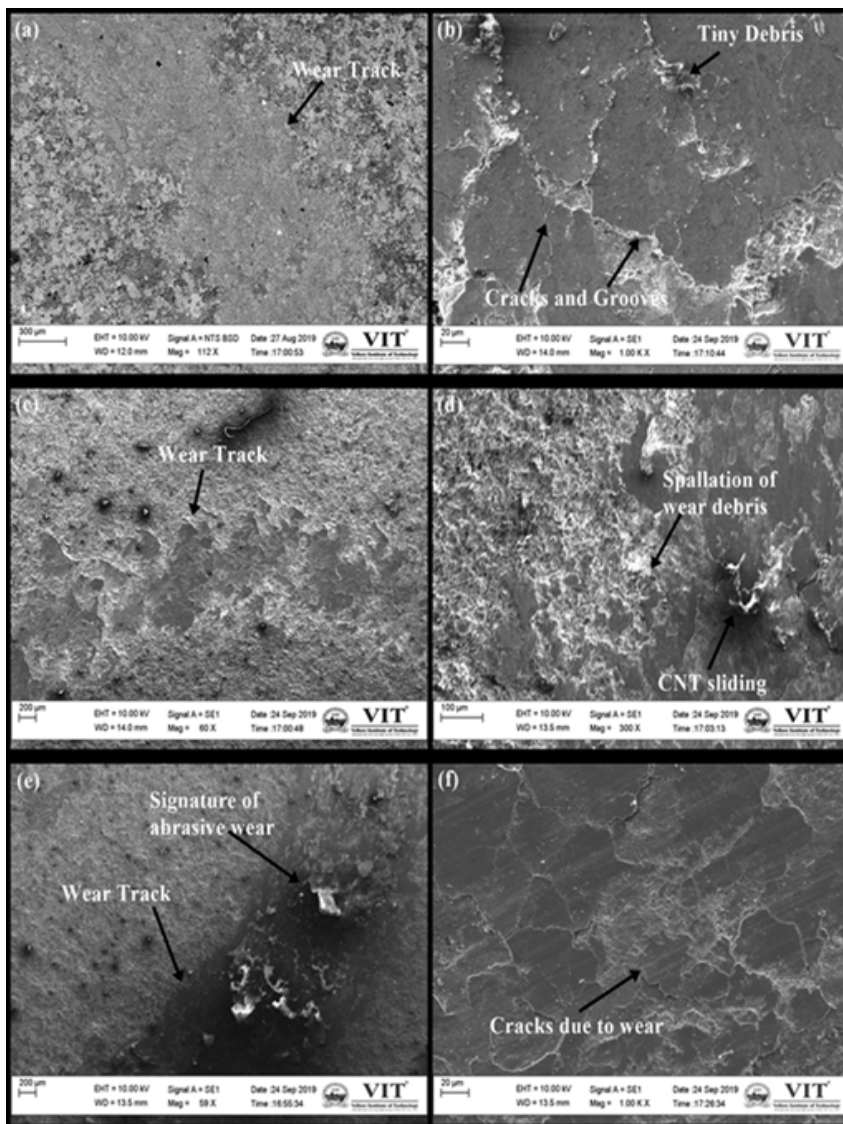


**Fig. 9.** Morphologies of wear track for Alumina-3wt% Titania coatings at different magnifications (a, b) Coatings obtained at 2wt% CNT, (c, d) Coatings deposited with 4wt% CNT and (e, f) Coatings deposited with 6wt% CNT. Results mentioned were for a load of 1.0kgf, Sliding speed of 0.5m/s, and at a sliding distance of 300metres.

imum load due to abrasive wear (see Fig. 8a) and material removal was less when compared to other loading conditions (see table 3) as the coating gets only rubbed against the WC ball. But for AT-4 coated samples, the cracks get deflected due to the presence of CNTs and it can be observed from Fig. 8 (d). The CNTs induced crack arresting mechanism can also be identified from this micrograph. In the case of 6wt % of CNTs (AT-6), the coating surface after wear test seem to have a tribofilm (an indication of the white color layer as shown in Fig.8 (e) which acts as a protective layer and reduces the coefficient of friction. This tribofilm occurs mainly due to the

presence of CNT bridging over  $Al_2O_3$  splats. Fig. 8f shows the stripping of wear debris in the wear track morphology and it can be due to the occurrence of unpuled CNTs on the wear track surface [34].

Likewise, the wear track morphologies for the other two sets of loading and speed conditions were shown in Fig. 9 (for 1.0 kgf at 0.33m/s sliding speed) and Fig. 10 (0.5 kgf at 0.5 m/s). For the AT-2 coated samples, the wear track morphology was seen to have cracks, grooves, and tiny debris spalling out from the coated surface (see Fig. 9 b). The grooves present in the track surface were due to the vertical impact of the WC ball over the surface.

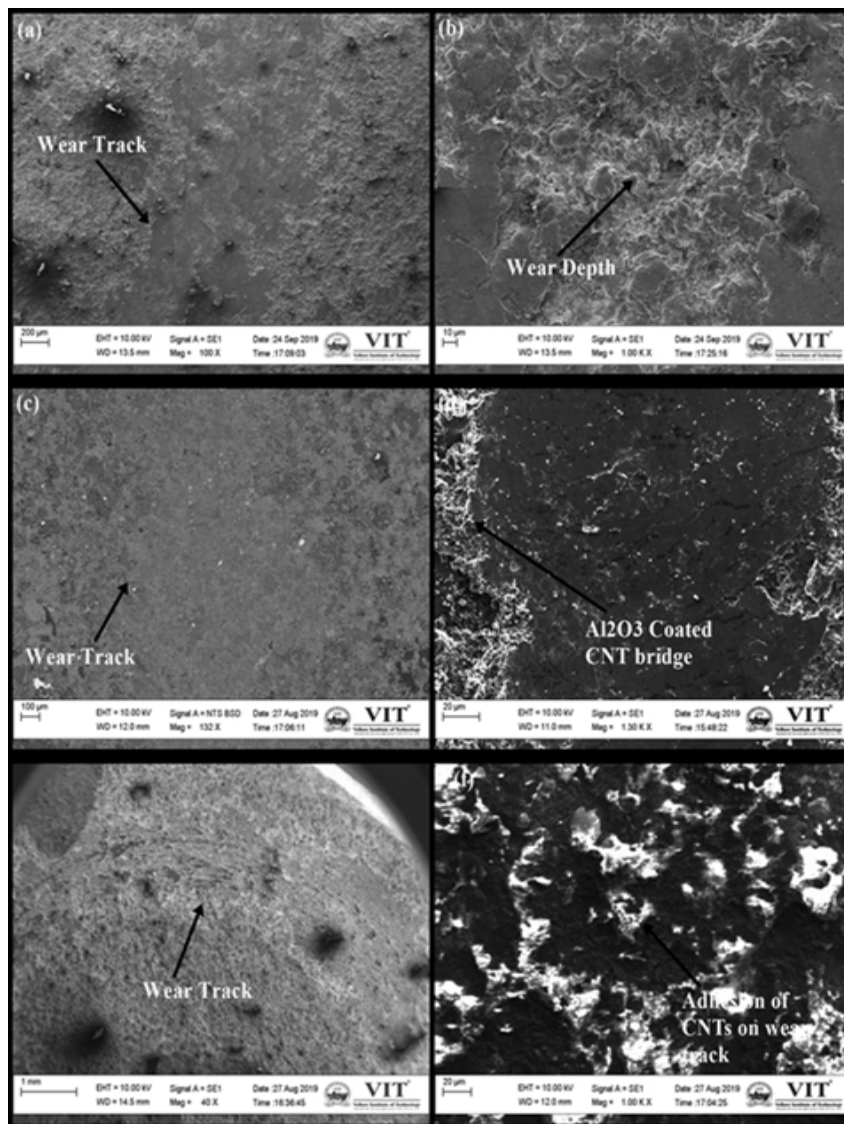


**Fig. 10.** Morphologies of wear track for Alumina-3wt% Titania coatings at different magnifications (a,b) Coatings obtained at 2wt% CNT, (c,d) Coatings deposited with 4wt% CNT and (e,f) Coatings deposited with 6wt% CNT. Results shown were for a normal load of 0.5kgf, Sliding velocity of 0.17m/s, and sliding distance of 300metres.

For AT-4 samples, the spallation of the coating was occurring due to the sliding of CNTs as shown in Fig. 9d. In AT-6 coated samples, the initiation of micro cracks were observed in the coating surface without much spallation of coating and resulting in less wear rate (see Fig. 9 f and table 3). It can also be seen that because of the increase in the percentage of CNT reinforcement, the pulverized debris due to wear was re-deposited which indicates the signature of abrasive wear (see Fig. 9 e). Furthermore, there was not much variation in wear mechanism and almost the wear was mainly due to the abrasion of particles from the coated surface.

The wear track morphologies on the worn-out surface at 0.5 kgf load and 0.5 m/s sliding speed of the coatings derived from 2wt%, 4wt%, and 6wt% CNTs were shown in Fig. 10 (a-f). For this testing conditions, the wear tracks were not formed clearly, but the wear rate and weight loss occurs at maximum level as compared to 1.5 kgf and 1.0 kgf loading conditions. The wear depth was slightly high as compared to the depth obtained at other loading conditions but at 0.5 kgf, the depth is significantly increasing (see Fig. 10 b). For AT-4 coated samples, the  $Al_2O_3$  coated CNT bridges were found across the splats (see Fig. 10 d). It can also be observed

that the wear tracks were in smooth condition for all the percentages of CNTs. Similarly, for AT-6 coated samples, the wear track was very slight and at higher magnification, it can be observed that the CNT particles mixed with  $\text{Al}_2\text{O}_3$ - $\text{TiO}_2$  powders get adhered to the wear track of the coating surface as shown in Fig. 10 (f).

#### 4. CONCLUSIONS

The  $\text{Al}_2\text{O}_3$ -3wt% $\text{TiO}_2$  coatings reinforced with 2wt%, 4wt%, and 6wt% CNTs were prepared using Air Plasma Spraying process and the following conclusions were made based on the results obtained from microstructural, mechanical, and tribological characteristics of coatings. The CNTs were present in the microstructure of the coatings even after undergone intense high-temperature spraying. It was found that the microhardness, porosity as well as surface roughness showed significant improvement. Similarly, the microstructural property also showing improvement i.e.,  $\text{Al}_2\text{O}_3$  coated CNT bridges in between the splats. The wear behavior analysis results showed that the wear tracks were clearly observed at 1.5 kgf and 1.0 kgf loading conditions. The wear track was very slight at 0.5 kgf loading due to less impact of WC ball over the coated surface. The detailed examination of the morphology of wear track shows that the abrasive wear mechanism is the primary wear mechanism involved. The  $\text{Al}_2\text{O}_3$ -3wt% $\text{TiO}_2$  coatings derived from 6wt% CNT and at 1.5 kgf loading condition showed less wear rate, less weight loss, and reduced coefficient of friction. From this work, it can be concluded that by adding CNTs to  $\text{Al}_2\text{O}_3$ -3wt%- $\text{TiO}_2$  up to 6wt%, the properties of coatings can be modified in a positive manner. Further, the future scope of this research work can be extended in such a way that instead of obtaining CNTs reinforced coatings, reduced graphene oxides (rGOs) can be used as reinforcement additives in order to obtain self-lubrication coatings and the same can be analyzed for various applications.

#### REFERENCES

- Balani, K., Agarwal, A., "Process Map for Plasma Sprayed Aluminum Oxide- Carbon Nanotube Nanocomposite Coatings". *J. Surf. Coat. Technol.*, 2008, 202, 4270-4277.
- Wang, Y., Jiang, S., Wang, M., Wang, S., Xiao, T. D. and Strutt, P. R., "Abrasive Wear Characteristics of Plasma Sprayed Nanostructured Alumina/Titania Coatings". *Wear*, 2000, 237, 176-185.
- Sarkariya, O., "Effect of Some Parameters on Microstructure and Hardness of Alumina Coatings prepared by the Air Plasma Spraying Process". *J. Surf. Coat. Technol.*, 2005, 190, 388-393.
- Bolleddu, V., Racherla, V. and Bandhyopadhyay, P. P., "Mechanical and Tribological Characterization of Air Plasma Sprayed Nanostructured Alumina-Titania Coatings deposited with nitrogen and argon as primary plasma gases". *Materials and Design*. 2014, 59, 252-263.
- Singh, L. and Chawla Grewal, J. S., "A Review on Detonation gun sprayed coatings". *J. Minerals & Materials Charac. & Engg.*, 2012, 11(3), 243-265.
- Hirlekar, R., Yamagar, M., Gharse, H., Vij, M. and Kadam, V., "Carbon Nanotubes its applications: review". *Asian J Pharm Clinical Research*, 2009, 2, 17-27.
- Mukherjee, B., Asiq Rahman, O. S., Sribalaji, M., Bakshi, S. R., Keshri, A. K., "Synergistic effect of carbon nanotube as sintering aid and toughening agent in spark plasma sintered molybdenum disilicide-hafnium carbide composite". *Mat.Sci. Eng, A-Struct.*, 2016, 678, 299-307.
- Cho, J. Y., Zhang, S. H., Cho, T. Y., Yoon, J. H., Joo, Y. K., Hur, S. K., "The processing optimization and property evaluations of HVOF Co-base alloy T800 coating". *J. Materials Science*, 2009, 44, 6348-6355.
- Vijayanand, P., Kumar, A., V., Kumar, K. R., Vinod, A., Kumaran P., Arungalai Vendan, S., "Characterizations of Plasma Sprayed Composite Coatings over 1020 Mild steel." *J. Mechanical Science and Tech.*, 2017, 31, 4747-4754.
- Mo, C. B., Cha, S. I., Kim, K. T., Lee, K. H., Hong, S. H., "Fabrication of carbon nanotube reinforced alumina matrix nanocomposite by sol-gel process". *Material Science Engg.* 2005, 395, 124-128.
- Cha, S. I., Kim, K. T., Lee, K. H., Mo, C. B., Hong, S. H., "Strengthening and toughening of carbon nanotube reinforced alumina nanocomposite fabricated by molecular level mixing process". *Ser. Mater.*, 2005, 53, 793-797.
- Keshri, A. K., Huang, J., Singh, V., Choi, W., Seal, S., Agarwal, A., "Synthesis of aluminum oxide coating with carbon nanotube reinforced produced by chemical vapor deposition for improved fracture and wear resistance". *Carbon*, 2010, 48, 431-442.
- Lei, S., Feng, Z. Y., Chan, Z., Ji, L., "Heterocoagulation system assisted adsorption of carbon nanotubes on alumina for toughening ceramics". *J. Re-*



- inforced Plastic Composites., 2008, 27, 245-253.
14. Lahiri, D., Singh, V., Keshri, A. K., Seal, S., Agarwal, A., "Carbon nanotube toughened hydroxyapatite by spark plasma sintering: Microstructural evolution and multiscale tribological properties". Carbon, 2011, 48, 3103-3120.
  15. Mehar, S., Sapate, S. G., Vashistha, N., Bagde, P., "Effect of Y2O3 addition on tribological properties of plasma sprayed Al2O3-13%TiO2 coating", Ceramis International, 2020.
  16. Wang, X., Feng, X., Lu, Ch., Yi, G., Jia, J., Li, H., "Mechanical and Tribological properties of plasma sprayed NiAl coatings with addition of nanostructured TiO2/Bi2O3", Surface&Coatings Technology, 2018, 349, 157-165.
  17. Psyllaki, P. P., Jandin, M., Pantelis, D. I., "Microstructure and wear mechanisms of thermal sprayed alumina coatings", Materials Letters, 2001, 47,77-82.
  18. Hawthorne, H. M., Erickson, L. C., Ross, D., Tai, H., Tronczynski, T., "The Microstructural dependence of wear and indentation behaviour of some plasma sprayed alumina coatings", Wear, 1997, 203-204, 709-714.
  19. Zhang, T., Kumari, L., Du, G. H., Li, W. Z., Wang, Q. W., Balani, K., Agarwal, A., "Mechanical properties of carbon nanotube-alumina nanocomposites synthesized by chemical vapour deposition and plasma sintering", Composites:Part A, 2009, 40, 86-93.
  20. Keshri, A. K., Huang, J., Choi, W. and Agarwal, A., "Intermediate Temperature Tribological Behavior of Carbon Nanotube Reinforced Plasma Sprayed Aluminum Oxide Coating". J. Surf. Coat. Technol., 2010, 204, 1847-1855.
  21. Ahmad, I., Kennedy, A. and Zhu, Y. Q., "Wear Resistant Properties of Multi Walled Carbon Nanotubes Reinforced Al2O3 Nanocomposites". Wear, 2010, 269, 71-78.
  22. An, J. W., You, D. H., and Lim, D. S., "Tribological Properties of Hot-Pressed Alumina-CNT Composites". Wear, 2003, 255, 677-681.
  23. Balani, K., Harimkar, S. P., Keshri, A. K., Chen, Y., Dahotre, N. B. and Agarwal, A., "Multiscale Wear of Plasma-Sprayed Carbon- Nanotube-Reinforced Aluminum Oxide Nanocomposite Coating". Acta Mater, 2008, 56, 5984-5994.
  24. Sudhakar C., Jambagi, P.P., Bandyopadhyay, "Improvement in Tribological properties of plasma-sprayed Alumina coatings upon carbon nanotube reinforcement", Journal of Materials Engineering and Performance, 2019.
  25. Jagadeeswaran, N., Ramesh, M. R., Udaya Bhat, K., "Oxidation resistance of HVOF sprayed coatings by 25% (Cr3C2-25(Ni20Cr)) + 75% NiCrAlY on titanium alloy." Procedia Materials Science, 2014, 5, 11-20.
  26. Fowler, D. B., Riggs, R., "Inspecting Thermal Sprayed Coatings". Advanced Mater Proc., 1990, 11, 41-52.
  27. Lamuta, C., Di Girolamo, G., Pagnotta, L., "Microstructural, mechanical and tribological properties of nanostructured YSZ coatings produced with different APS process parameters." Ceramics International, 2015, 41(7), 8904-8914.
  28. Thakare, J. G., Mulik, R. S., Mahapatra, M. M., "Effect of carbon nanotubes and aluminum oxide on the properties of a plasma sprayed thermal barrier coating." Ceramics International, 2017.
  29. Aruna, S., Balaji, N., Shedthi, J., Grips, V. W., "Effect of critical plasma spray parameters on the microstructure, microhardness and wear and corrosion resistance of plasma sprayed alumina coatings". J. Surf. Coat and Technol., 2012, 208, 92-100.
  30. Ranjan, Sh., Mukherjee, B., Islam, A., Pandey, K. K., Gupta, R., Keshri, A. K., "Microstructural, Mechanical and high temperature tribological behaviour of Graphene nanoplatelets reinforced plasma sprayed titanium nitride coating" The Journal of European Ceramic Society, 2019.
  31. Ariharan, S., Nisar, A., Balaji, N., Aruna, S. T., Balani, K., "Carbon nanotubes stabilize high temperature phase and toughen Al2O3-based thermal barrier coatings". Composites Part B, 2017, 124, 76-87.
  32. Liutauras Maranauskas, Jacob Shiby Mathew, Mindaugas Mileska, Balakumaran Thanigachalam, Alja Kupec, Ramunas Cesnavicius, Romualdas Kezelis, Mitjan Kalin, "Microstructure and Tribological properties of plasma sprayed alumina and alumina-graphite coatings", Journal of Surface Coatings & Technology, 2018.
  33. Rong, J., Yang, K., Zhuang, Y., Zhao, H., Liu, Ch., Tao, S. Y., Ding, Ch., "Comparative tribological study of plasma sprayed alumina and alumina-ytria under severe conditions", Surface Coatings & Technology, 201.
  34. Belmonte, M., Ramirez, C., González-Julián, J., Schneider, J., Miranzo, P., Osendi, M. I., "The beneficial effect of graphene nanofillers on the tribological performance of ceramics". Carbon, 2013, 61, 431-5.